



HAL
open science

Multiscale Passive Mechanical Characterization of Rodent Skeletal Muscle

P. Pouletaut, Y. Tatarenko, M.K. Chakouch, M. Li, V. Joumaa, J.R. Hawse,
W. Herzog, S. Chatelin, S.F. Bensamoun

► **To cite this version:**

P. Pouletaut, Y. Tatarenko, M.K. Chakouch, M. Li, V. Joumaa, et al.. Multiscale Passive Mechanical Characterization of Rodent Skeletal Muscle. *Innovation and Research in BioMedical engineering*, 2023, 44 (6), pp.100800. 10.1016/j.irbm.2023.100800 . hal-04212727v2

HAL Id: hal-04212727

<https://hal.science/hal-04212727v2>

Submitted on 3 Oct 2023

HAL is a multi-disciplinary open access archive for the deposit and dissemination of scientific research documents, whether they are published or not. The documents may come from teaching and research institutions in France or abroad, or from public or private research centers.

L'archive ouverte pluridisciplinaire **HAL**, est destinée au dépôt et à la diffusion de documents scientifiques de niveau recherche, publiés ou non, émanant des établissements d'enseignement et de recherche français ou étrangers, des laboratoires publics ou privés.

Multiscale Passive Mechanical Characterization of Rodent Skeletal Muscle

P. Pouletaut¹, Y. Tatarenko^{1,4}, M.K. Chakouch¹, M. Li², V. Joumaa², J.R. Hawse³, W. Herzog²,
S. Chatelin⁴, S.F. Bensamoun^{1,*}

¹Sorbonne University, Université de Technologie de Compiègne, CNRS UMR 7338, Biomechanics and Bioengineering, Compiègne, France

²University of Calgary, Faculty of Kinesiology, Human Performance Laboratory, Calgary, Alberta, Canada

³Department of Biochemistry and Molecular Biology, Mayo Clinic, Rochester, MN, USA

⁴ICube, CNRS UMR 7357, University of Strasbourg, Strasbourg, France

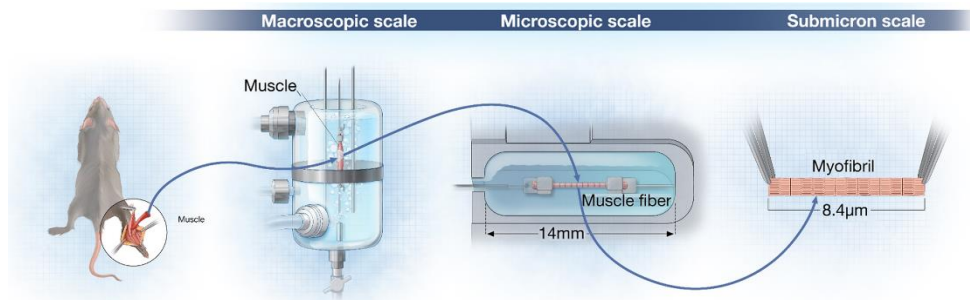
* Correspondence and requests for materials should be addressed to S.F.B.
(Email:sabine.bensamoun@utc.fr)

Université de Technologie de Compiègne (UTC)
Laboratoire Biomécanique et Bioingénierie - UMR CNRS 7338
Rue Roger Couitolenc
CS 60319
60203 Compiègne cedex
France
Tel: (33) 03 44 23 43 90

Highlights

- Comparison of elastic properties for slow- and fast-twitch muscles at three scales
- Significant passive mechanical differences only observed at the macroscopic scale
- Characterization of passive mechanical behavior at the macro/micro/submicron scales
- This study provides referent data to the multiscale muscle literature

Graphical abstract



Characterization of passive mechanical behavior for slow (soleus) and fast (extensor digitorum longus) twitch muscles at macro/micro/submicron scales

Abstract

Purpose: To experimentally measure selected passive properties of skeletal muscle at three different scales (macroscopic scale: whole muscle, microscopic scale: single skinned fiber, and submicron scale: single myofibril) within the same animal model (mice), and to compare a primarily slow-twitch fiber muscle (soleus) and a primarily fast-twitch fiber muscle (extensor digitorum longus, EDL) for each scale.

Methods: Healthy 3 month-old wild-type C57BL6 mice were used. To characterize each scale, soleus (N = 11), EDL (N = 9), slow fibers (N = 17), fast fibers (N = 16), and myofibrils from soleus (N = 11) and EDL (N = 11) were harvested. Passive mechanical (ramp, relaxation) tests were applied at each scale to compare the passive properties (Young's modulus, static and dynamic stresses) within a given scale, across scales and between muscle types.

Results: The soleus and EDL showed significant passive mechanical differences at the macroscopic scale while no variation was observed between both tissues at the microscopic and submicron scales. The results highlight the importance of the scale that is used to mechanically characterize a multiscale tissue.

Conclusion: The present work will allow for a better understanding of the multiscale passive mechanical properties for two muscles with vastly differing physiological and metabolic properties. This study provides referent data to the body of literature that can be built upon in future work.

Keywords: mice, elastic properties, myofibril, fiber, soleus/EDL

1. Introduction

Skeletal muscle is a complex tissue divided into four main scales [1,2]: 1) the macroscopic scale (whole muscle diameter: about 1-3 cm for mice), 2) the mesoscopic scale (single fascicle diameter: about 0.5-30 mm), 3) the microscopic scale (single muscle fiber diameter: 10-100 μm), and 4) the submicron scale (single myofibril diameter: about 1-3 μm). All structural elements contribute to the overall mechanical response of the muscle.

The majority of mechanical studies performed on skeletal muscle from rodents have focused on the characterization at one scale. Indeed, the analysis of each muscle scale requires specific equipment which is difficult to house and maintain, and necessitates personnel with the corresponding expertise. *In vitro* testing of different muscle components is commonly performed with mechanical devices enabling the longitudinal stretching of an entire muscle [3], single fibers [4] or myofibrils [5-7]. Other experimental techniques, such as atomic force microscopy [8,9] and elastography [10] are used to provide the transverse local elastic modulus and longitudinal stiffness, respectively.

An efficient way to describe the global behavior of the muscle, through its different scales, is to represent the muscle by a finite element model [11,12] including a cost law composed of experimental multiscale parameters. In the literature, analytical and numerical homogenization methods have been used to analyze biological tissues at different structural levels, for example the myocardium [13] and skeletal muscles [14]. These models, based on experimental data, illustrated the importance of each scale on the global tissue response, and the difficulty to experimentally determine the mechanical properties at each scale of interest. The present study aimed to characterize the passive mechanics of skeletal muscle at different structural levels to inform how scaling might vary by muscle type (slow-twitch vs fast-twitch fiber muscles), an issue that is largely neglected in multiscale modeling approaches. This study also provides referent data to the multiscale muscle literature that can be used by all investigators to build upon.

Thus, the novelty of the present study was 1) to experimentally measure selected passive properties at three different scales (whole muscle, single skinned fiber, and single myofibril) within the same animal model (mice), and 2) to compare a primarily slow-twitch fiber muscle (soleus) and a primarily fast-twitch fiber muscle (extensor digitorum longus, EDL) for each scale. The present work provides a better understanding of the multiscale passive mechanical properties for two muscles with vastly differing physiological and metabolic properties.

2. Materials and Methods

All of the following mechanical tests were performed with the same initial sarcomere length for all specimens at the different scales (approximately for muscles), but with different strains, taken from the literature, and corresponding to the behavior of the living tissues.

2.1. Animals

We used healthy 3 month-old wild-type female mice (C57BL/6). Animals were maintained at 22 ± 2 °C with a light/dark cycle of 12 hours, and they had free access to food and water. The protocol was approved by the French ethics committee (CREMEAP; Permit Number: APAFIS #8905-2021011109249708).

2.2. Passive mechanical tests performed at the macroscopic scale

Soleus and EDL were harvested from the left hindlimb, placed in a bath containing a physiological Ringer's solution ($T = 25$ °C; pH 7.3; 95 % O_2 and 5 % CO_2) and the proximal and the distal ends were connected to a dual mode force transducer (300C-LR dual-mode muscle lever, Aurora Scientific, Ontario, Canada) and to a hook, respectively (Fig. 1). Software (ASI610A Dynamics Muscle Control v5.420, Aurora Scientific, Ontario, Canada) was used to control displacement of the lever arm to stretch the muscle at different velocities. Prior to testing, the muscle was placed at its optimal length corresponding to the maximum contraction

force developed by the muscle [15], and pre-conditioned with two stretch-release cycles, spaced 5 min apart [16,17].

After resting for 5 min, soleus and EDL muscles underwent a ramp test (Fig. 2A) with a stretch-release cycle consisting of a stretch of 25 % of optimal length ($L_o \approx 10$ mm) at a velocity of 1.67 % $L_o.s^{-1}$ (about 0.167 mm.s⁻¹) followed by a release at the same velocity, allowing the measurement of the static force (F_{s_Ramp}) reached at the maximum of the stretch.

The force-displacement curve was recorded and the stress-strain curve was generated to measure the Young's modulus (E) in the linear part of the loading curve between 60 and 80 % of the applied stretch [18].

Following an additional 5 min rest, the viscoelastic behavior was characterized through a stress-relaxation test using a fast stretch velocity of 5 $L_o.s^{-1}$ (about 50 mm.s⁻¹) with a stretch amplitude of 25 % L_o , and held at the final length for 250 s. Two parameters were measured: 1) the dynamic force (F_d) corresponding to the maximum force of the muscle reached at the end of the stretch, and 2) the static force (F_{s_Relax}) corresponding to the steady state force reached at the end of the holding period. The cross-sectional area was calculated for the soleus and the EDL using the equation of Del Prete et al. (2008) [19] and the forces were normalized to anatomical cross-sectional area to determine the dynamic (σ_d) and static (σ_{s_Ramp} , σ_{s_Relax}) stress.

2.3. Passive mechanical tests performed at the microscopic scale

Skinned muscle fibers were isolated from soleus and EDL muscles as previously described [20]. Each fiber was placed in a small bath filled with a relaxing solution (70 mM potassium propionate, 8 mM magnesium acetate, 5 mM EGTA, 7 mM ATP, 6 mM Imidazole, 10 mM PMSF, 50 mg.L⁻¹, Trypsin inhibitor, 4 mg.L⁻¹ Leupeptine, pH = 7.1) [21]. Each fiber was set at a sarcomere length of 2.4 μ m and its slack length ($L_s \approx 2$ mm) and diameter were then measured. Subsequently, each fiber underwent two preconditioning tests [20] followed by two passive mechanical tests (ramp stretch, stress-relaxation).

For the preconditioning test, each fiber was stretched with a stretch amplitude of 50 % L_s (about 1 mm) at velocity of $0.00167 L_s.s^{-1}$ (about $3.33 \mu m.s^{-1}$) and relaxed at the same velocity. After 5 min of rest, this preconditioning test was repeated twice. The hysteresis loop was plotted for each preconditioning run. The hysteresis area was calculated, and a minimum decrease of 10 % in the hysteresis area was used to determine whether the steady state was achieved [22]. Of note, the minimum decrease was always achieved in the second hysteresis test.

The first passive mechanical test was a ramp stretch (Fig. 2B) performed with a stretch with an stretch amplitude of 50 % L_s (about 1 mm) with a velocity of $0.033 L_s.s^{-1}$ (about $66 \mu m.s^{-1}$) and released at the same velocity, allowing the measurement of the static force (F_{s_Ramp}) reached at the maximum of the stretch. From the stress-strain curve, the Young's modulus (E) was measured in the linear part of the loading curve between 60 and 80 % of the applied stretch [18] .

The second passive mechanical test was a relaxation test in which the fiber was rapidly elongated with a stretch amplitude of 50 % L_s (about 1 mm) at a high velocity of $3.3 L_s.s^{-1}$ (about $6.6 mm.s^{-1}$) and released to its slack length after a 60 s hold at 50 % strain. The dynamic force F_d , corresponding to the maximal force value, reached at the end of the stretch, and the static force F_{s_Relax} measured at the end of the test, before the fiber was released, were determined.

Forces were divided by the anatomical cross-sectional area of the fiber to obtain the dynamic σ_d and static (σ_{s_Ramp} , σ_{s_Relax}) stresses.

2.4. Submicron scale

A small piece (about 5 mm in length and 2 mm in width) of additional soleus and EDL skinned muscles was placed in a microcentrifuge tube containing rigor solution and vortexed to separate individual myofibrils [4]. Then, myofibrils were fixed under an inverted microscope to a glass needle attached to a length controller at one end, and to a nanolever at the other end

(Fig. 1), allowing for length changes and force measurements, respectively [4]. The striation pattern of the myofibrils was projected onto a linear photodiode array for determination of individual sarcomere lengths. The diameter of the myofibrils was measured at a magnification of 40X and used to determine the cross-sectional area of the myofibril. Myofibrils were set at an average sarcomere length of 2.4 μm and a stress-relaxation test was performed.

The myofibrils were passively stretched (Fig. 2C) at a velocity of 0.1 $\mu\text{m}\cdot\text{s}^{-1}$ to an average sarcomere length of 3.4 μm corresponding to a strain of 40 %. The stretch was held for 20 seconds until a steady-state force was reached, and then released. Passive force reached at steady-state was determined and converted to stress by dividing force by the cross-sectional area of the myofibril.

2.5. Statistical analysis

The SystatTM V11 (Systat Software Inc., CA, USA) was used and non-parametric two-sample Mann-Whitney tests were performed to compare the various parameters. Results were considered significant for $p\text{-value} < 0.05$.

3. Results

At the macroscopic scale (Tables 1 and 2), significant differences were identified for the passive parameters ($\sigma_{\text{s_Ramp}}$, $\sigma_{\text{s_Relax}}$, σ_{d}) between the soleus and EDL muscles. The ramp test revealed a significant higher value of the static stress for the soleus ($\sigma_{\text{s_Ramp}} = 209.8 \pm 13.8$ kPa) compared to the EDL ($\sigma_{\text{s_Ramp}} = 83.7 \pm 6.5$ kPa, $p < 0.001$). The Young's modulus (E) was significantly greater for the soleus ($E = 1.21 \pm 0.10$ MPa) compared to EDL ($E = 0.52 \pm 0.06$ MPa, $p < 0.001$). Similarly, the dynamic stress has significantly higher value for the soleus ($\sigma_{\text{d}} = 307.6 \pm 18.7$ kPa) compared to the EDL ($\sigma_{\text{d}} = 134.4 \pm 10.8$ kPa, $p < 0.001$).

At the microscopic scale (Tables 1 and 2), fibers from the EDL had a small higher value ($p = 0.13$ and 0.264) in the static and dynamic stresses ($\sigma_{s_Ramp} = 286.7 \pm 34.0$ kPa, $\sigma_d = 396.9 \pm 47.1$ kPa) compared to the fibers from the soleus ($\sigma_{s_Ramp} = 212.6 \pm 20.4$ kPa, $\sigma_d = 305.6 \pm 26.1$ kPa). The Young's modulus was slightly lower ($p = 0.264$) for the soleus ($E = 0.60 \pm 0.06$ MPa) compared to the EDL fibers ($E = 0.86 \pm 0.13$ MPa). The static stress (σ_{s_Relax}), obtained with the relaxation test, was slightly lower ($p = 0.195$) for the soleus compared to the EDL fibers. None of these observed differences are statistically significant.

At the submicron scale (Tables 1 and 2), the soleus myofibrils had a non-significant slight higher value in the passive stress (about 9 kPa) compared to the EDL myofibrils ($p = 0.364$).

4. Discussion

The originality of the present study was to compare a slow-twitch (soleus) and fast-twitch (EDL) muscle at three different scales. Interestingly, the soleus and EDL showed significant passive mechanical differences at the macroscopic scales while no variation was observed between both tissues at the microscopic and submicron scales. The comparison of the present data with the literature remains difficult due to the various experimental protocols applied for the different mechanical tests which leads to different 1) mechanical parameters (strain rate,...), 2) rodents (rabbit, rat), 3) tissue preparations (fresh vs skinned), 4) composition of the physiological solutions, etc. However, some studies can be cited; the macroscopic results of our study follow the same tendency found by Hakim et al. (2011) and Anderson et al. (2001) where the dynamic stress (about 400 kPa, [23]) for the EDL (from 2 months age) at 25 % of strain was lower (625 kPa [24]) than that of the soleus (from 5 months age) at 25 % strain. The results of our study highlight the importance of the scale that is used to mechanically characterize a multiscale tissue.

It is assumed that the mechanical changes, found at the macroscopic level, are related to the extracellular matrix (ECM) which is well known to have an effect on muscle structural properties [25-26]. For example, Rowe et al. (2010) [27] demonstrated that collagenase digestion of ECM has an impact on the passive elastic properties of the diaphragm. Moreover, Brashear et al. [28] showed that the structural organization of the collagen fibers within the ECM impacts the mechanical properties of the tissue. In addition, several studies [29-30] have demonstrated that slow-twitch muscles have a larger amount of collagen (mainly composed of type 1 and type 3) than fast-twitch muscles, which could explain the higher rigidity found in the present study for the soleus compared to EDL at the macroscopic level.

Future directions of this work will be to improve the experimental protocol using the same amplitude of strain for all specimens and to include the assessment of the mesostructure scale corresponding to the fascicle tissue. It should be noted that this scale has been poorly analyzed (Meyer et al., 2011) [31]. However, the present study provides a first step of challenging experimental and numerical studies which will help to answer the following questions: how is the macroscopic mechanical behavior of the muscle impacted by its microscopic and submicroscopic properties? and to what extent can we link the latter in order to predict its evolution?

5. Conclusion

This study provides the mechanical properties of two types of muscle at three different scales in the same animal model. The results indicate different mechanical responses depending on the scale of tissue being analyzed. These data could provide a framework for investigators to prioritize the most appropriate scale for their studies of interest.

Conflict of interest statement

All authors have no conflict of interest to disclose.

Financial support

This work was supported by IDEX Sorbonne University SU-19-3-EMRG-12, the Research Department of UTC within the framework of AMI International and the National Institutes of Health, Grant No. R01 DE14036 (to J.R.H.). This work of the Interdisciplinary Thematic Institute ITI HealthTech was supported by IdEx Unistra (ANR-10-IDEX-0002) and SFRI (STRAT'US project, ANR-20-SFRI-0012).

Acknowledgements

We would also like to thank Frank Corl of the Mayo Clinic for the artistic rendering provided in Figure 1.

References

- [1] Tatarenko, Y., Pouletaut, P., Chatelin, S., Bensamoun, S.F., 2022. Passive and active mechanical tests at different scales of the skeletal muscle: a literature review. *State of the Art in Bioengineering* 2.
- [2] Bensamoun, S., Stevens, L., Fleury, M.J., Bellon, G., Goubel, F., Ho Ba Tho, M.C., 2006. Macroscopic–microscopic characterization of the passive mechanical properties in rat soleus muscle. *Journal of Biomechanics* 39, 568–578. <https://doi.org/10.1016/j.jbiomech.2004.04.036>
- [3] Anderson, J., Li, Z., & Goubel, F., 2002. Models of skeletal muscle to explain the increase in passive stiffness in desmin knockout muscle. *Journal of biomechanics*, 35(10), 1315–1324. [https://doi.org/10.1016/S0021-9290\(02\)00170-7](https://doi.org/10.1016/S0021-9290(02)00170-7)
- [4] Joumaa, V., Rassier, D.E., Leonard, T.R., Herzog, W., 2008. The origin of passive force enhancement in skeletal muscle. *American Journal of Physiology-Cell Physiology* 294, C74–C78. <https://doi.org/10.1152/ajpcell.00218.2007>
- [5] Linke, W.A., 2000. Stretching molecular springs: elasticity of titin filaments in vertebrate striated muscle. *Histol Histopathol* 15, 799–811. <https://doi.org/10.14670/HH-15.799>
- [6] Herzog, W., 2014. The role of titin in eccentric muscle contraction. *Journal of Experimental Biology* 217, 2825–2833. <https://doi.org/10.1242/jeb.099127>
- [7] Powers, K., Joumaa, V., Jinha, A., Moo, E.K., Smith, I.C., Nishikawa, K., Herzog, W., 2017. Titin force enhancement following active stretch of skinned skeletal muscle fibers. *Journal of Experimental Biology* 220, 3110–3118. <https://doi.org/10.1242/jeb.153502>
- [8] Kammoun, M., Ternifi, R., Dupres, V., Pouletaut, P., Mème, S., Mème, W., Szeremeta, F., Landoulsi, J., Constans, J.-M., Lafont, F., Subramaniam, M., Hawse, J.R., Bensamoun, S.F., 2019. Development of a novel multiphysical approach for the characterization of mechanical properties of musculotendinous tissues. *Sci Rep* 9, 7733. <https://doi.org/10.1038/s41598-019-44053-1>
- [9] Canato, M., Dal Maschio, M., Sbrana, F., Raiteri, R., Reggiani, C., Vassanelli, S., Megighian, A., 2010. Mechanical and Electrophysiological Properties of the Sarcolemma

- of Muscle Fibers in Two Murine Models of Muscle Dystrophy: Col6a1 and Mdx. *Journal of Biomedicine and Biotechnology* 2010, e981945. <https://doi.org/10.1155/2010/981945>
- [10] Ternifi, R., Kammoun, M., Pouletaut, P., Subramaniam, M., Hawse, J.R., Bensamoun, S.F., 2020. Ultrasound image processing to estimate the structural and functional properties of mouse skeletal muscle. *Biomedical Signal Processing and Control* 56, 101735. <https://doi.org/10.1016/j.bspc.2019.101735>
- [11] Wheatley, B.B., Morrow, D.A., Odegard, G.M., Kaufman, K.R., Haut Donahue, T.L., 2016. Skeletal muscle tensile strain dependence: Hyperviscoelastic nonlinearity. *Journal of the Mechanical Behavior of Biomedical Materials* 53, 445–454. <https://doi.org/10.1016/j.jmbbm.2015.08.041>
- [12] Wheatley, B.B., 2017. Finite element analysis of skeletal muscle: a validated approach to modeling muscle force and intramuscular pressure (Doctoral dissertation). Colorado State University. <http://hdl.handle.net/10217/181381>
- [13] Tueni, N., Allain, J.-M., Genet, M., 2022. On the structural origin of the anisotropy in the myocardium: Multiscale modeling and analysis. <https://hal.archives-ouvertes.fr/hal-03604234>
- [14] Spyrou, L.A., Brisard, S., Danas, K., 2019. Multiscale modeling of skeletal muscle tissues based on analytical and numerical homogenization. *Journal of the Mechanical Behavior of Biomedical Materials* 92, 97–117. <https://doi.org/10.1016/j.jmbbm.2018.12.030>
- [15] Barton, E. R., Lynch, G., Khurana, T. S., Raymackers, J.-M., Dorchie, O., & Carlson, G., 2008. Measuring isometric force of isolated mouse muscles in vitro. *Exp Protoc DMD Anim Model Treat-NMD Neuromuscul Network*, 1(2), 14.
- [16] Canon, F., Gamet, D., Perot, C., 2008. Passive stiffness of rat soleus muscle from weaning to senescence. *Computer Methods in Biomechanics and Biomedical Engineering* 11, 49–50. <https://doi.org/10.1080/10255840802296756>
- [17] Toscano, A.E., Ferraz, K.M., de Castro, R.M., Canon, F., 2010. Passive stiffness of rat skeletal muscle undernourished during fetal development. *Clinics* 65, 1363–1369. <https://doi.org/10.1590/S1807-59322010001200022>
- [18] Hollenstein, M., Nava, A., Valtorta, D., Snedeker, J.G., Mazza, E., 2006. Mechanical Characterization of the Liver Capsule and Parenchyma, in: Harders, M., Székely, G. (Eds.), *Biomedical Simulation, Lecture Notes in Computer Science*. Springer, Berlin, Heidelberg, pp. 150–158. https://doi.org/10.1007/11790273_17
- [19] Del Prete, Z., Musarò, A., Rizzuto, E., 2008. Measuring Mechanical Properties, Including Isotonic Fatigue, of Fast and Slow MLC/mIgf-1 Transgenic Skeletal Muscle. *Ann Biomed Eng* 36, 1281–1290. <https://doi.org/10.1007/s10439-008-9496-x>
- [20] Kammoun, M., Pouletaut, P., Morandat, S., Subramaniam, M., Hawse, J. R., & Bensamoun, S. F., 2021. Krüppel-like factor 10 regulates the contractile properties of skeletal muscle fibers in mice. *Muscle & Nerve*, 64(6), 765-769. <https://doi.org/10.1002/mus.27412>
- [21] Joumaa, V., Fitzowich, A., & Herzog, W., 2017. Energy cost of isometric force production after active shortening in skinned muscle fibres. *Journal of Experimental Biology*, 220(8), 1509-1515. <https://doi.org/10.1242/jeb.117622>
- [22] Kammoun, M., Pouletaut, P., Canon, F., Subramaniam, M., Hawse, J.R., Vayssade, M., Bensamoun, S.F., 2016. Impact of TIEG1 Deletion on the Passive Mechanical Properties of Fast and Slow Twitch Skeletal Muscles in Female Mice. *PLOS ONE* 11, e0164566. <https://doi.org/10.1371/journal.pone.0164566>
- [23] Hakim, C. H., Grange, R. W., & Duan, D., 2011. The passive mechanical properties of the extensor digitorum longus muscle are compromised in 2- to 20-month-old mdx mice. *Journal of applied physiology*, 110(6), 1656-1663. <https://doi.org/10.1152/jappphysiol.01425.2010>
- [24] Anderson, J., Li, Z., & Goubel, F., 2001. Passive stiffness is increased in soleus muscle

- of desmin knockout mouse. *Muscle & Nerve: Official Journal of the American Association of Electrodiagnostic Medicine*, 24(8), 1090-1092. <https://doi.org/10.1002/mus.1115>
- [25] Csapo, R., Gumpenberger, M., & Wessner, B. (2020). Skeletal muscle extracellular matrix—what do we know about its composition, regulation, and physiological roles? A narrative review. *Frontiers in physiology*, 11, 253. <https://doi.org/10.3389/fphys.2020.00253>
- [26] Gillies, A. R., Chapman, M. A., Bushong, E. A., Deerinck, T. J., Ellisman, M. H., & Lieber, R. L., 2017. High resolution three-dimensional reconstruction of fibrotic skeletal muscle extracellular matrix. *The Journal of physiology*, 595(4), 1159-1171. <https://doi.org/10.1113/JP273376>
- [27] Rowe, J., Chen, Q., Domire, Z.J., McCullough, M.B., Sieck, G., Zhan, W.-Z., An, K.-N., 2010. Effect of collagen digestion on the passive elastic properties of diaphragm muscle in rat. *Medical Engineering & Physics* 32, 90–94. <https://doi.org/10.1016/j.medengphy.2009.11.002>
- [28] Brashear, S. E., Wohlgemuth, R. P., Gonzalez, G., & Smith, L. R., 2021. Passive stiffness of fibrotic skeletal muscle in mdx mice relates to collagen architecture. *The Journal of physiology*, 599(3), 943-962. <https://doi-org.ezproxy.utc.fr/10.1113/JP280656>
- [29] Miller, T. A., Lesniewski, L. A., Muller-Delp, J. M., Majors, A. K., Scalise, D., & Delp, M. D., 2001. Hindlimb unloading induces a collagen isoform shift in the soleus muscle of the rat. *American Journal of Physiology-Regulatory, Integrative and Comparative Physiology*, 281(5), R1710-R1717. <https://doi.org/10.1152/ajpregu.2001.281.5.R1710>
- [30] Riso, E. M., Kaasik, P., & Seene, T., 2016. Remodelling of skeletal muscle extracellular matrix: effect of unloading and reloading. *Composition and function of the extracellular matrix in the human body*, 45-68. <https://doi-org/10.5772/62295>
- [31] Meyer, G.A., Lieber, R.L., 2011. Elucidation of extracellular matrix mechanics from muscle fibers and fiber bundles. *Journal of Biomechanics* 44, 771–773. <https://doi.org/10.1016/j.jbiomech.2010.10.044>

Tables Captions List

Table 1.

For the (A) macroscopic, (B) microscopic and (C) submicron scales, static stress (σ_{s_Ramp} , σ_{s_Relax}), dynamic stress (σ_d), and Young's modulus (E) values (mean \pm sem) obtained with the ramp and relaxation tests on soleus and extensor digitorum longus (EDL) mice muscles.

Table 2.

P-value from Mann-Whitney's test for the comparison between soleus and EDL, of the static stress (σ_{s_Ramp} , σ_{s_Relax}), dynamic stress (σ_d), and Young's modulus (E) for the three structural levels with ramp and relaxation tests.

Table 1**(A) Macroscopic scale**

	σ_{s_Ramp} (kPa)	E (kPa)	σ_{s_Relax} (kPa)	σ_d (kPa)
Soleus (n = 11)	209.8 ± 13.8	1.21 ± 0.10	123.7 ± 7.3	307.6 ± 18.7
EDL (n = 9)	83.7 ± 6.5	0.52 ± 0.06	47.5 ± 3.8	134.4 ± 10.8

(B) Microscopic scale

	σ_{s_Ramp} (kPa)	E (kPa)	σ_{s_Relax} (kPa)	σ_d (kPa)
Soleus (n = 17)	212.6 ± 20.4	0.60 ± 0.06	108.9 ± 11.0	305.6 ± 26.1
EDL (n = 16)	286.7 ± 34.0	0.86 ± 0.13	147.5 ± 19.9	396.9 ± 47.1

(C) Submicron scale

	σ_{s_Ramp} (kPa)
Soleus (n = 11)	51.8 ± 6.3
EDL (n = 11)	42.5 ± 4.7

Table 2

	σ_{s_Ramp}	E	σ_{s_Relax}	σ_d
Macroscopic scale (soleus vs EDL)	< 0.001	< 0.001	< 0.001	< 0.001
Microscopic scale (soleus vs EDL)	0.130	0.264	0.195	0.264

	σ_{s_Ramp}
Submicron scale (soleus vs EDL)	0.364

Figures Captions List

Fig. 1. Representation of the mechanical tests performed on healthy murine muscles at the macroscopic (muscle), microscopic (fiber) and submicron (myofibril) levels.

Fig. 2. Representative stress vs time curves for an exemple ramp test (left side) and an exemple relaxation test (middle side with a zoom of the initial stress on the right side), at the macroscopic (A), microscopic (B) and submicron (C) scales from soleus and EDL tissues. The curve in the thin line represents the strain of the tissue. EDL: extensor digitorum longus. For the ramp test, the velocities were 0.167 mm.s^{-1} , $66 \text{ }\mu\text{m.s}^{-1}$, $0.1 \text{ }\mu\text{m.s}^{-1}$ for muscle, fiber and myofibril, respectively. For the relaxation test, the velocities were 50 mm.s^{-1} and 6.6 mm.s^{-1} for muscle and fiber, respectively.

Fig. 1

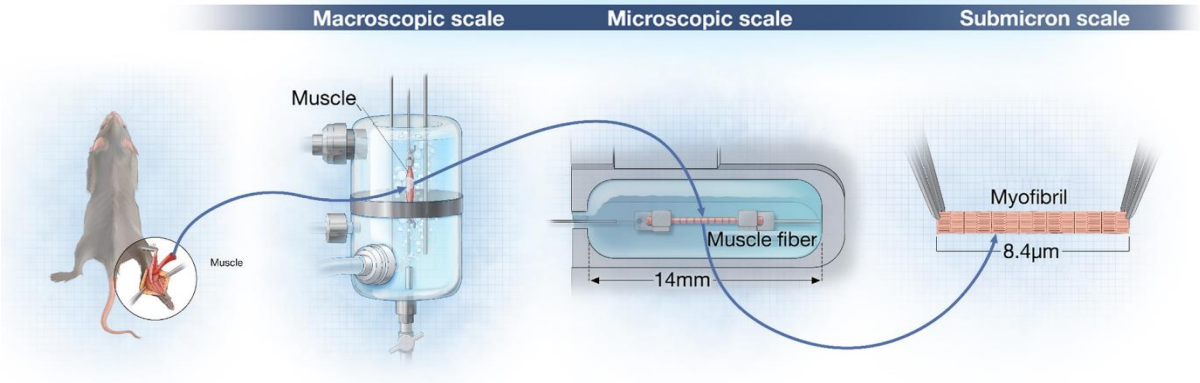
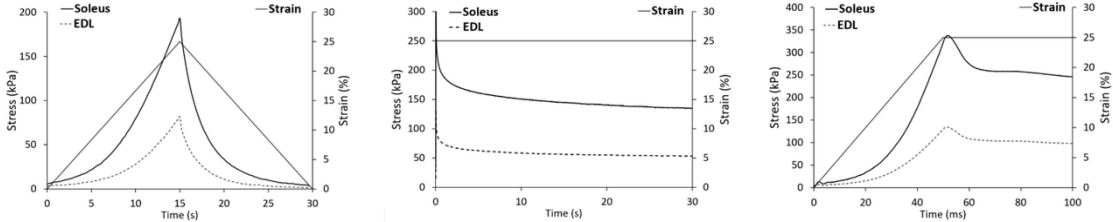
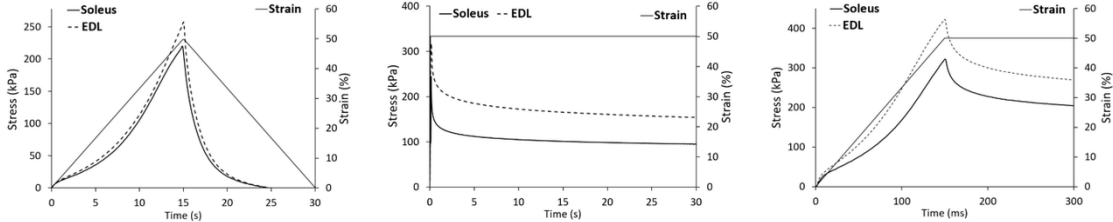


Fig. 2

(A) Macroscopic scale



(B) Microscopic scale



(C) Submicron scale

